Early Detection of Glaucoma from Cropped Fundus Images Using Transfer-Learned Convolutional Neural Network

Md Faisal Karim
Department of Computer Science & Engineering
Rajshahi University Of Engineering & Technology
itsfaisalkarim@gmail.com

Md Ali Hossain
Department of Computer Science & Engineering
Rajshahi University Of Engineering & Technology
ali.hossain@cse.ruet.ac.bd

Azmain Yakin Srizon
Department of Computer Science & Engineering
Rajshahi University Of Engineering & Technology
azmainsrizon@gmail.com

Nazmul Haque
Department of Computer Science & Engineering
Rajshahi University Of Engineering & Technology
nazmulruetcse18@gmail.com

***Abstract*—Glaucoma, a major contributor to irreversible blindness, which requires early diagnosis and appropriate treatment. In this work, we use deep learning techniques to automate the diagnosis of glaucoma from retinal fundus images. For increased efficiency, we use a cropped fundus images instead of analyzing entire fundus photos. We use VGG-19, ResNet-50, and EfficientNet B3 for binary classification on the ACRIMA dataset. Notably, ResNet-50 achieves 100% accuracy. Next, we combine glaucoma suspect samples from publicly accessible datasets with ACRIMA and DRISHTI-GS1 to create "Glaucoma suspect" class in a custom multiclass dataset. Using this dataset, EfficientNet-B3 and ResNet-50 produce 97% and 98% accuracy rates, respectively. Both models perform flawlessly when it comes to categorizing the suspect class & negative class with 100% sensitivity. Our results highlight the effectiveness of deep learning in glaucoma detection and provide interesting directions for enhancing diagnostic precision and facilitating early intervention.**

***Index Terms*—Glaucoma, Early detection, Cropped, Fundus, Transfer learning**

I. Introduction

Glaucoma, a leading cause of irreversible blindness [22], is projected to affect 111.8 million people globally by 2040 [21]. This progressive optic nerve disease often develops without symptoms, making early detection crucial to prevent permanent vision loss. Traditional diagnostic methods are subjective and labor-intensive, highlighting the need for automated, accurate, and efficient detection systems.

The objective of our research is to create a deep learning technique that utilizes cropped fundus photos to diagnose glaucoma early, focusing on the optic disk and cup region. We utilize VGG-19, ResNet-50, and EfficientNet-B3 models for binary classification on the ACRIMA dataset, with ResNet-50 achieving 100% accuracy. Additionally, we create a multiclass dataset incorporating glaucoma suspect samples, achieving high accuracy rates. Our results demonstrate the potential of deep learning to enhance glaucoma screening and diagnosis.

II. Related works

The literature review underscores glaucoma's impact on vision and surveys machine learning and deep learning in its automated diagnosis. Research shows different methods for automated glaucoma detection with different datasets and techniques. While some papers focus solely on machine learning, deep learning predominates in the majority, often in combination with other techniques.

Using a novel dataset, Islam et al. (2022) [23] suggested an automated classification strategy that makes use of deep learning models, yielding excellent accuracy. Kurilová et al. (2023) [2] investigated the use of ensemble learning methodologies and single CNN models for glaucoma detection, highlighting the efficacy of group approaches. A public dataset for glaucoma pattern recognition was presented by Bragança et al. (2022) [3], who demonstrated encouraging outcomes using deep learning frameworks. Tekouabou et al. (2021) [4] highlighted the potential of ensemble classifiers by presenting a three-step classification strategy for early glaucoma identification. Using pre-trained CNNs, Velpula and Sharma (2023) [5] present an automated glaucoma classification model. They validate it on four datasets, highlighting its potential for early glaucoma detection. Key contributions include a three-class classification framework, classifier fusion, and thorough validation. An automated glaucoma diagnostic system using HOS cumulants retrieved from RT on fundus pictures is proposed by Noronha et al. (2014) [1]. Using the NB classifier, they attain an average accuracy of 92.65% for all classes and 84.72% for early detection when classifying glaucoma into three categories: normal, mild, and moderate/severe. The system shows promise for mass glaucoma screening.

Elangovan et al. (2022) [6] used the strengths of various CNN architectures to propose a deep ensemble model for glaucoma detection. Using pre-trained CNNs, Deepa et al.

(2022) [7] presented a comprehensive learning system for glaucoma identification that outperformed individual models. In order to achieve excellent accuracy and recall rates in automated glaucoma diagnosis, Mahdi et al. (2022) [8] proposed an architecture based on CNN. A deep learning ensemble approach was presented by Cho et al. (2021) [9] for glaucoma severity grading, which outperformed single CNN models in classification accuracy. All things considered, Deep learning algorithms offer promise in automating glaucoma diagnosis.

III. Methods

Here is the methodology flowchart of our work.

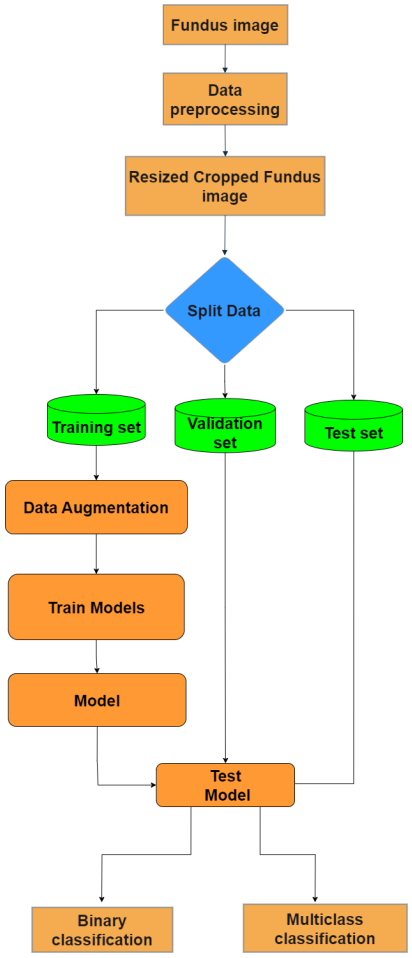

Fig. 1: Proposed Methodology

A. Dataset Description

In our study, we conducted both binary and multiclass classification tasks. For binary classification, we utilized the ACRIMA [14] dataset, comprising 326 glaucomatous samples and 239 non-glaucomatous samples.

For multiclass classification, we employed a custom dataset with three distinct labels: Glaucoma, Non-glaucoma, and Glaucoma suspect. This dataset was created by amalgamating binary labeled samples from the ACRIMA and DRISHTI-GS1 [10] datasets, along with 133 samples labeled as 'Glaucoma suspect' sourced from five additional datasets. Specifically, the ACRIMA dataset contributed 326 Glaucoma and 239 non-glaucoma samples, while the DRISHTI-GS1 dataset added 70 Glaucoma and 31 non-glaucoma samples.

Additionally, we collected 133 'Glaucoma suspect' samples from various datasets: 68 from Papila [11], 13 from JSIEC-1000 [12], 18 from OIA-ODIR [13] TRAIN, 25 from OIA-ODIR TEST-ONLINE, and 9 from OIA-ODIR TEST-OFFLINE. These samples were sourced from the SMDG-19 dataset [15] collection, available on Kaggle. So in total, 799 samples including 396 Glaucomaic, 270 Non-glaucomatic and 133 Suspect samples.

B. Data Preprocessing

Retinal fundus image preprocessing involved several steps to align with the requirements of selected pre-trained deep learning models. Initially, full fundus images were manually cropped using the 'Pinetools' online tool to isolate the optic disk and cup region. Subsequently, the cropped images were resized to dimensions compatible with the input size of the chosen pre-trained models, typically 300×300 or 224×224 pixels. A significant portion of the samples was sourced from a dataset collection named SMDG-19, already preprocessed and standardized, thereby significantly reducing the preprocessing workload.

The resizing process mathematically can be represented as follows:

1) I_{orig} denotes the original fundus image with dimensions $W_{\text{orig}} \times H_{\text{orig}}$.
2) After cropping, I_{crop} with dimensions $W_{\text{crop}} \times H_{\text{crop}}$ is obtained.
3) I_{crop} is resized to desired dimensions $W_{\text{resize}} \times H_{\text{resize}}$ using bilinear interpolation.

The resizing operation is given by:

$$I_{\text{resized}} = \text{resize}(I_{\text{crop}}, (W_{\text{resize}}, H_{\text{resize}})) \quad (1)$$

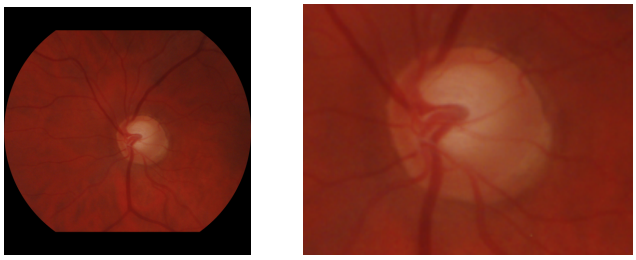

(a) Full fundus image (b) Cropped fundus image

Fig. 2: Fundus image preprocessing

These procedures guarantee that fundus images are ready for the next stage of feature extraction and deep learning model classification.

C. Data Augmentation

Following a random partitioning of the dataset into test, validation, and training sets (80:10:10) for multiclass classification and 80:20 for binary classification (where the test and validation sets are the same), we augmented the training set. In total, we utilized 3000 images after augmentation, with 1000 images per class for multiclass classification and 2000 total training images for binary classification, maintaining a balance of 1000 images per class. The primary objective of augmentation was to address class imbalance, which was prevalent in our dataset. Here are some of the techniques we used for augmentation:

TABLE I: Augmentation Techniques and Parameter Values

Augmentation Technique	Parameter Value
Rotation	$\pm 10^{\circ}$
Width Shift	0.1
Height Shift	0.1
Shear	0.15
Zoom	0.1
Channel Shift	10.
Horizontal Flip	True

D. Setting the Models

Throughout our efforts, transfer learning has been applied. The ImageNet database [16] was used to train each of these models. In total, we trained 3 different pre-trained models. VGG-19 [17], ResNet-50 [18] & EfficientNet-B3 [19] were trained for binary classification. ResNet-50, EfficientNet-B3 was trained for multiclass classification.

First, we load pre-trained weights from ImageNet into the pre-trained model, and then we freeze the last layer. To generate extra parameters from our dataset, we build a custom head. It varies from model to model. We used a Global Average Pooling Layer followed by a dense layer with a 'ReLu' activation function. Convolutional neural networks (CNNs) use the Global Average Pooling (GAP) layer to shrink the spatial dimensions of feature maps without losing critical information. Mathematically, the output of the GAP layer can be computed as follows:

$$\text{GAP}(X_{ijc}) = \frac{1}{H \times W} \sum_{i=1}^{H} \sum_{j=1}^{W} X_{ijc} \tag{2}$$

In all three of the binary classification models, we used the identical Dropout of 0.5, a dense layer of 1 unit, and a'sigmoid' activation function.

We first employed a global average pooling layer in multiclass classification, followed by a dense layer using the 'ReLu' activation function. With many classes to be classified, the next dense layer is composed of three units with a 'softmax' activation function. Overfitting was the main issue for the training model on that dataset as it is more diverse. So we used L2 regularization with a factor of 0.01 in both dense layers. The regularization term is a function of the weights' squared magnitude.

$$\text{L2\_regularization\_term} = \lambda \sum_{i=1}^{n} w_i^2 \tag{3}$$

where:

- λ is the regularization parameter, controlling the strength of regularization.
- w_i represents the weights in the model.
- n is the total number of weights in the model.

We used dynamic learning rate, which was defined by a custom function function consisting of some conditional statements. 'Adam' was the optimizer used to compile the model. Because of its processing efficiency, we chose it. We only trained the custom head, so the initial layers of those models were set to non-trainable. For binary classification, we employed "Binary Cross-Entropy (BCE)" as the loss function, while for multiclass classification, we utilized "Categorical Cross-Entropy (CCE)".

The binary cross-entropy loss function is defined as:

$$\text{BCE} = -\frac{1}{N} \sum_{i=1}^{N} \left(y_i \cdot \log(p_i) + (1 - y_i) \cdot \log(1 - p_i) \right) \tag{4}$$

The categorical cross-entropy loss function is defined as:

$$\text{CCE} = -\frac{1}{N} \sum_{i=1}^{N} \sum_{j=1}^{C} y_{ij} \cdot \log(p_{ij}) \tag{5}$$

We used several metrics to monitor during training. Accuracy, AUC, precision, recall, specificity and sensitivity. During training, we evaluated 'validation loss' as the core parameter.

E. Hyperparameters Settings

We evaluated different kinds of hyperparameter settings to properly fit the model. In all cases, we used 256 dense units. In the case of binary classification, the batch size is 64 and in the multiclass classification, we used a batch size of 32. Another important hyperparameter is the learning rate. We used different learning rate schedules for every model as per the model's accuracy and loss curve. Most of the time we used a decay in learning rate as the epoch goes on. We implemented the early stopping, model checkpoint, ReduceLROnPlateau in the case of multiclass classification. Regularization and early stopping helped greatly to avoid overfitting in model training.

F. Training of the Models

We set the initial epoch number as 200 in the case of multiclass but for binary classification, it was less than 30 epochs. Throughout training, our goal was to optimize the validation loss metric, which serves as a crucial indicator of model performance and generalization ability. By monitoring validation loss, we ensured that the models were not overfitting to the training data and were capable of effectively capturing relevant patterns in the dataset.

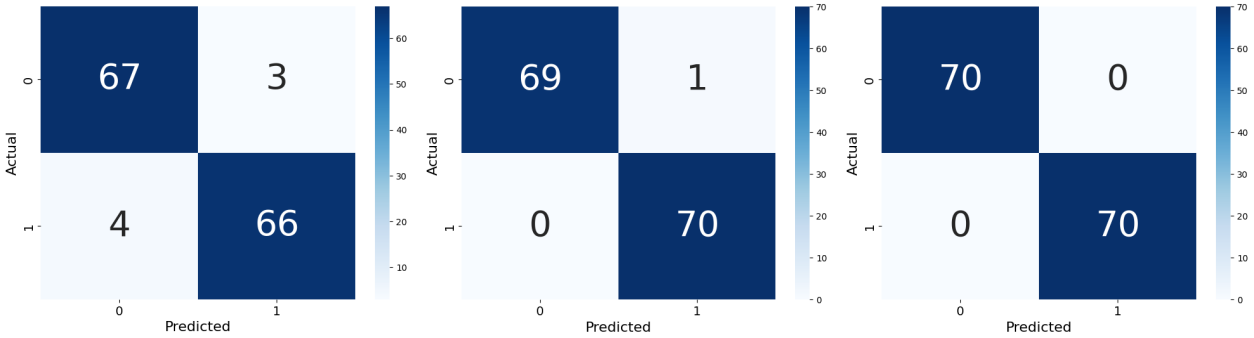

(a) CM for VGG-19 (b) CM for EfficientNet-B3 (c) CM for ResNet-50

Fig. 3: Confusion Matrices of different studied Models

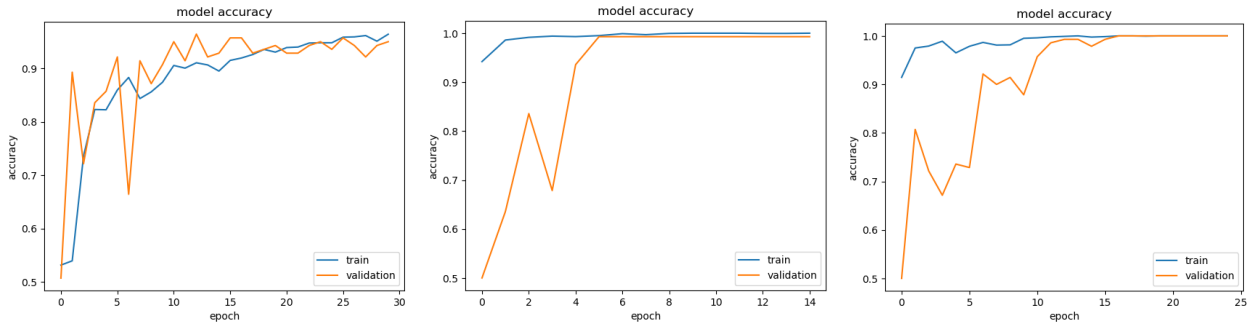

(a) Accuracy curve for VGG-19 (b) Accuracy curve for EfficientNet-B3 (c) Accuracy curve for ResNet-50

Fig. 4: Accuracy curve for Various Models(Binary classification)

IV. Results

A. Binary Classification

In Binary classification we trained 3 pre-trained model named VGG-19, EfficientNet-B3, ResNet-50. Table 2 elaborates the best result for each models.

TABLE II: Performance Metrics of Various Models

Models	Accuracy	F1 Score	Precision	Sensitivity
EfficientB-3	0.99	0.99	1.00	0.99
Resnet-50	1.00	1.00	1.00	1.00
VGG-19	0.95	0.95	0.94	0.96

The rigorous analysis of model performance sheds light on their effectiveness, aiding in informed decision-making for future endeavors in image classification. EfficientNet-B3 exhibited outstanding performance, boasting a remarkable accuracy of 99% and an F1 score of 99%. With a precision of 100% and a sensitivity of 99%, the model showcased excellent predictive capability. It employed standard configurations, including a gradual learning rate schedule and dropout regularization, and underwent training for 15 epochs. ResNet-50 demonstrated impeccable performance, achieving a flawless accuracy of 100% and an F1 score of 100%. With perfect precision and sensitivity metrics, both at 100%, the model showcased exemplary classification prowess. Similar to EfficientNet-B3, it adhered to a standard learning rate schedule and employed dropout regularization, undergoing training for 25 epochs. VGG-19 displayed commendable performance, attaining a respectable accuracy of 95% and an F1 score of 95%. While precision slightly trailed at 94%, sensitivity remained relatively high at 96%. Employing a similar learning rate schedule and dropout regularization, the model underwent training for 30 epochs.

In conclusion, the performance of all models showcased remarkable results, with ResNet-50 emerging as the undisputed leader, closely trailed by EfficientNet-B3. Despite its marginally lower scores, VGG-19 still showcased commendable performance, reaffirming the effectiveness of deep learning architectures in the realm of image classification tasks.

B. Multiclass Classification

In Multiclass classification, we trained ResNet-50 and EfficientNet B3 using a custom dataset. Due to limited publicly available suspect samples in a single dataset, we gathered samples from multiple sources. Suspect samples were taken from five distinct datasets and combined with the DRISHTI-GS1 dataset from ACRIMA.

EfficientNet-B3 impressively classifies glaucoma cases with 97% accuracy. Its flawless precision in identifying glaucoma and suspect cases minimizes false positives. Despite slightly lower sensitivity for glaucoma cases, it maintains perfect sensitivity for non-glaucoma and suspect instances. High F1

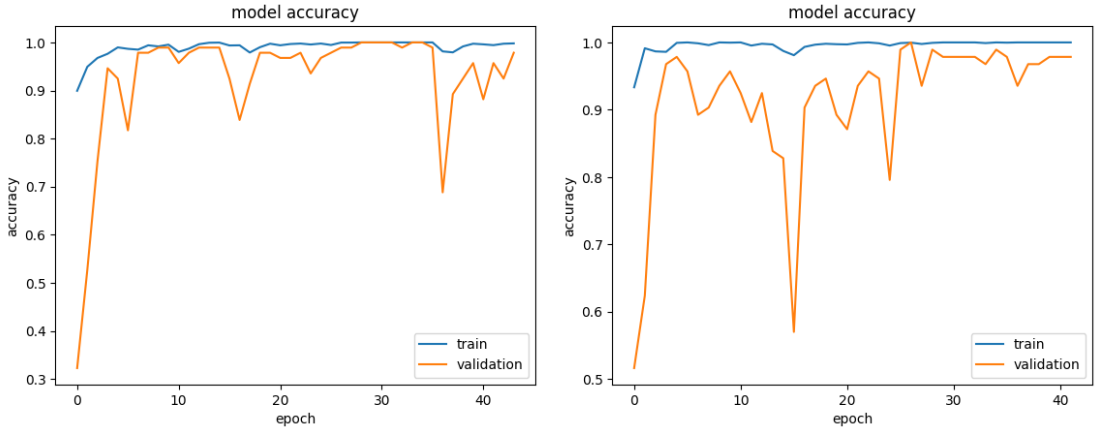

(a) Accuracy curve for EfficientNet-B3 (b) Accuracy curve for ResNet-50

Fig. 5: Accuracy curves for Various Models

TABLE III: Accuracy Comparison of EfficientNet-B3 and ResNet-50

Models	Accuracy
EfficientNet B-3	0.97
ResNet50	0.98

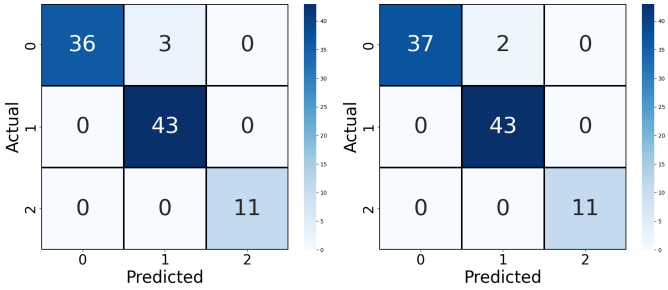

(a) CM For EfficientNet-B3 (b) CM For ResNet-50

Fig. 6: Confusion Matrices of Different Studied Models

scores across all classes showcase a balanced approach between precision and sensitivity. Training involves a dynamic learning rate schedule over 200 epochs with a batch size of 32, utilizing callbacks like EarlyStopping and ModelCheckpoint. The model's training concludes at the 44th epoch, with the best model achieved at epoch 29.

ResNet-50 outperforms EfficientNet-B3 with a 98% accuracy. It exhibits perfect precision and sensitivity across all classes, ensuring precise classification and effective identification of positive instances. High F1 scores highlight its robust performance in glaucoma detection. L2 regularization, dynamic learning rate scheduling, and Adam optimizer contribute to its training settings. Trained over 200 epochs with a batch size of 32, ResNet-50 utilizes similar callbacks, stopping at the 42nd epoch, with the best model achieved at epoch 27.

In comparison, ResNet-50 shows slightly higher accuracy than EfficientNet-B3. However, both models achieve comparable performance metrics, with negligible differences in precision, sensitivity, and F1 scores. The choice between the two may depend on specific requirements, such as computational efficiency or model interpretability. Nevertheless, meticulously designed training settings and effective callbacks significantly contribute to both models' remarkable performance in glaucoma detection.

TABLE IV: Performance Metrics of Glaucoma Detection Models

Model	Metrics	Positive	Negative	Suspect
EfficientNet-B3	Precision	1.00	0.93	1.00
	Sensitivity	0.92	1.00	1.00
	F1 Score	0.96	0.97	1.00
ResNet-50	Precision	1.00	0.96	1.00
	Sensitivity	0.95	1.00	1.00
	F1 Score	0.97	0.98	1.00

V. Comparision with other works

Both binary & multiclass classification was intoduced in our work. Here in a table we compared our work with some other related works on the same topic.

TABLE V: A Comparition with different works

Authors	Datasets	Models used	Best results
Islam et al. [23]	ACRIMA (two class)	EfficientNet-B3	Acc:99%
Proposed work	ACRIMA (two class)	VGG-19, ResNet-50, EfficientNet-B3	Acc:95%, **Acc:100%** , Acc:99%
Noronha et al. [1]	Private(three class)	SVM, NB	Acc:92.65%;
Vijaya et al. [5]	Relabelled Dhrishti-gs1(three class)	Combining ResNet-50, AlexNet, VGG-19	Acc:90.55%;
Proposed work	Custom Dataset (three class)	EfficientNet-B3, ResNet-50	Acc:97%, **Acc:98%**

VI. Discussion

To adapt these models for clinical use as a Computer-Aided Diagnostic (CAD) tool, extensive clinical trials are needed to validate the model's robustness across diverse patient populations. It is essential to integrate with current clinical procedures and electronic health record (EHR) systems. This would enable automated flagging of potential glaucoma cases for further examination by ophthalmologists. The workflow involves data acquisition through standard fundus cameras, preprocessing for quality consistency, model inference for classification, and clinical decision-making based on the CAD tool's output. Implementing these steps can significantly support clinicians in early glaucoma detection and management, improving patient outcomes.

VII. Conclusion & Future work

In our study, we focused on early glaucoma detection by creating a multiclass custom dataset from various public sources, introducing the 'Glaucoma Suspect' class as a key indicator. We performed binary and multiclass classifications using several pre-trained models, with ResNet-50 achieving 100% accuracy in binary and 98% in multiclass classifications, effectively identifying suspect class samples.Ensembling can improve classification performance on imbalanced datasets by combining predictions from multiple models. However, we chose not to use ensembling in this study to maintain focus on the individual performance of deep learning models like ResNet-50, which achieved high accuracy. Additionally, ensembling increases computational complexity and resource requirements, which may not be practical in clinical settings. Instead, we employed data augmentation and model optimization to address class imbalance. Future research should enhance model performance through diverse datasets, fine-tuning, and integrating multimodal data. Real-world clinical deployment and prospective studies will validate the model's clinical utility, advancing automated glaucoma diagnosis and patient care.

References

[1] K. P. Noronha, U. R. Acharya, K. P. Nayak, R. J. Martis, & S. V. Bhandary, "Automated classification of glaucoma stages using higher order cumulant features", Biomedical Signal Processing and Control, 10, 174–183, (2014, March), https://doi.org/10.1016/j.bspc.2013.11.006

[2] V. Kurilová, S. Rajcsányi, Z. Rábeková, J. Pavlovičová, M. Oravec, and N. Majtánová, "Detecting glaucoma from fundus images using ensemble learning," Journal of Electrical Engineering, vol. 74, p. 328–335, Aug 2023.

[3] C. P. Bragança, J. M. Torres, C. P. Soares, and L. O. Macedo, "Detection of glaucoma on fundus images using deep learning on a new image set obtained with a smartphone and handheld ophthalmoscope," Healthcare, vol. 10, p. 2345, Nov 2022.

[4] C. S. Koumetio Tekouabou, E. A. ABDELLAOUI ALAOUI, I. Chabbar, W. Cherif, and S. Hassan, "Using deep features extraction and ensemble classifiers to detect glaucoma from fundus images," pp. 63–70, 01 2021

[5] V. K.Velpula & L. D. Sharma (2023, June 13). Multi-stage glaucoma classification using pre-trained convolutional neural networks and voting-based classifier fusion. Frontiers in Physiology, 14. https://doi.org/10.3389/fphys.2023.1175881.

[6] P. Elangovan and M. K. Nath, "enconvnet: A novel approach for glaucoma detection from color fundus images using ensemble of deep convolutional neural networks," Inter- national Journal of Imaging Systems and Technology, vol. 32, p. 2034–2048, May 2022.

[7] N. Deepa, S. Esakkirajan, B. Keerthiveena, and S. B. Dhanalakshmi, "Automatic diagno- sis of glaucoma using ensemble based deep learning model," vol. 1, pp. 536–541, 2021.

[8] M. M. Mahdi, M. A. Mohammed, H. Al-Chalibi, B. S. Bashar, H. A. Sadeq, and T. M. J. Abbas, "An ensemble learning approach for glaucoma detection in retinal images," Dec 2022.

[9] H. Cho, Y. H. Hwang, J. K. Chung, K. B. Lee, J. S. Park, H.-G. Kim, and J. H. Jeong, "Deep learning ensemble method for classifying glaucoma stages using fundus photographs and convolutional neural networks," Current Eye Research, vol. 46, p. 1516–1524, Apr 2021.

[10] Sivaswamy, Jayanthi, S. R. Krishnadas, G. Ramakrishna Dutt, Joshi, Madhulika Jain, Ujjwal Syed and Tabish A. "Drishti-GS: Retinal image dataset for optic nerve head(ONH) segmentation." 2014 IEEE 11th International Symposium on Biomedical Imaging (ISBI) (2014): 53-56.

[11] O. Kovalyk, J. Morales-Sánchez, R. Verdú-Monedero, I. Sellés-Navarro, A. Palazón- Cabanes, and J.-L. Sancho-Gómez, "Papila: Dataset with fundus images and clinical data of both eyes of the same patient for glaucoma assessment," Scientific Data, vol. 9, no. 1, p. 291, 2022.

[12] Cen, LP., Ji, J., Lin, JW. et al. Automatic detection of 39 fundus diseases and conditions in retinal photographs using deep neural networks. Nat Commun 12, 4828 (2021). https://doi.org/10.1038/s41467-021-25138-w

[13] Li, N., Li, T., Hu, C., Wang, K., Kang, H. (2021). A Benchmark of Ocular Disease Intelligent Recognition: One Shot for Multi-disease Detection. In: Wolf, F., Gao, W. (eds) Benchmarking, Measuring, and Optimizing. Bench 2020. Lecture Notes in Computer Science(), vol 12614. Springer, Cham.https://doi.org/10.1007/978-3-030-71058-3_11

[14] A. Diaz-Pinto, S. Morales, V. Naranjo, T. Kohler, J. M. Mossi, and A. Navea, "Cnns for automatic glaucoma assessment using fundus images: an extensive validation," Biomedical engineering online, vol. 18, no. 1, pp. 1–19, 2019.

[15] Riley Kiefer, Muhammad Abid, Jessica Steen, Mahsa Raeisi Ardali, and Ehsan Amjadian. 2023. A Catalog of Public Glaucoma Datasets for Machine Learning Applications: A detailed description and analysis of public glaucoma datasets available to machine learning engineers tackling glaucoma-related problems using retinal fundus images and OCT images. In Proceedings of the 2023 7th International Conference on Information System and Data Mining (ICISDM '23). Association for Computing Machinery, New York, NY, USA, 24–31. https://doi.org/10.1145/3603765.3603779

[16] J. Deng, W. Dong, R. Socher, L. -J. Li, Kai Li and Li Fei-Fei, "ImageNet: A large-scale hierarchical image database," 2009 IEEE Conference on Computer Vision and Pattern Recognition, Miami, FL, USA, 2009, pp. 248-255, doi: 10.1109/CVPR.2009.5206848. keywords: Large-scale systems;Image databases;Explosions;Internet;Robustness;Information retrieval;Image retrieval;Multimedia databases;Ontologies;Spine.

[17] Simonyan, Karen & Zisserman, Andrew. (2014). Very Deep Convolutional Networks for Large-Scale Image Recognition. arXiv 1409.1556.

[18] K. He, X. Zhang, S. Ren and J. Sun, "Deep Residual Learning for Image Recognition," 2016 IEEE Conference on Computer Vision and Pattern Recognition (CVPR), Las Vegas, NV, USA, 2016, pp. 770-778, doi: 10.1109/CVPR.2016.90. keywords: Training;Degradation;Complexity theory;Image recognition;Neural networks;Visualization;Image segmentation.

[19] Mingxing Tan, V. Le. Quoc "EfficientNet: Rethinking Model Scaling for Convolutional Neural Networks." arXiv preprint arXiv:1905.11946 (2020).

[20] R. Janani, S.P. Rajamohana, Early detection of glaucoma using optic disc and optic cup segmentation: A survey, Materials Today: Proceedings, Volume 45, Part 2, 2021, Pages 2763-2769, ISSN 2214-7853, https://doi.org/10.1016/j.matpr.2020.11.613. (https://www.sciencedirect.com/science/article/pii/S2214785320392877)

[21] Quigley HA, Broman ATThe number of people with glaucoma worldwide in 2010 and 2020British Journal of Ophthalmology 2006;90:262-267.

[22] Quigley, H.A. and Broman, A.T., 2006. The number of people with glaucoma worldwide in 2010 and 2020. British journal of ophthalmology, 90(3), pp.262-267.

[23] M. T. Islam, S. T.Mashfu, A.Faisal, S. C.Siam, I. T.Naheen & R. Khan(2022). Deep Learning-Based Glaucoma Detection With Cropped Optic Cup and Disc and Blood Vessel Segmentation. IEEE Access, 10, 2828–2841. https://doi.org/10.1109/access.2021.3139160